Electronic Supporting Information

A novel cerium-based metal-organic framework supported Pd catalyst for semi-hydrogenation of phenylacetylene

Xiangdi Zeng,[a] Zi Wang,[a] Meng He,[a] Wanpeng Lu,[a] Wenyuan Huang,[b] Bing An,[a] Jiangnan Li,[b] Mufan Li,[b] Ben F. Spencer,[c] Sarah J. Day,[d] Floriana Tuna,[a,e] Eric J. L. McInnes,[a] Martin Schröder[a*] and Sihai Yang[a,b*]

a. Department of Chemistry, University of Manchester, Manchester, M13 9PL, UK. M.Schroder@manchester.ac.uk

b. College of Chemistry and Molecular Engineering, Beijing National Laboratory for Molecular Sciences, Peking University, Beijing, 100871, China. Sihai.Yang@pku.edu.cn

c. Department of Materials, The University of Manchester, Manchester, M13 9PL, UK.

d. Diamond Light Source, Harwell Science Campus, Didcot, Oxfordshire, OX11 0DE, UK.

e. Photon Science Institute, University of Manchester, Manchester, M13 9PL, UK.

Materials: All the reagents were commercially available from Sigma-Aldrich Chemical Co. Ltd. and used as such without further purification.

Experiment:

Powder X-ray diffraction

Powder X-ray diffraction (PXRD) patterns were recorded using a Philips X'pert X-ray diffractometer (40 kV and 30 mA) using Cu Kα radiation (λ = 1.5406 Å).

Brunauer-Emmett-Teller (BET) measurement

Gas sorption experiment was conducted using the Micrometric Tristar II plus. In a typical gas sorption experiment, the sample was activated under dynamic vacuum at 60 ^{o}C for 12 hours. Then the N_2 adsorption isotherm was measured at 77 K. The BET surface area and pore size distribution (PSD) plots were calculated by the software incorporated in the Micrometric Tristar II plus.[1,2]

Elemental Analysis

Elemental analysis for C, H and N content of complexes was carried out using a CE-440 Elemental Analyser manufactured by Exeter Analytical. Element analysis for Ce was carried out using ICP-OES measurements on a Perkin-Elmer Optima 2000.

Thermogravimetric analysis (TGA) Measurements

Thermogravimetric analysis was carried out under a flow of air (5 mL min^{-1}) with a heating rate of 5 °C min^{-1} on a Perkin-Elmer Pyris1 Thermogravimetric analyser. TGA data for Ce-bptc is shown in Figure S10.

X-ray photoelectron spectroscopy (XPS) measurement

XPS spectra were measured using a Kratos Axis Ultra instrument equipped with a monochromatic Al Kα X-ray source ($h\nu$ = 1486.6 eV). A charge neutraliser was used to minimise charging and spectra are aligned on the binding energy scale relative to the hydrocarbon C-C/C-H peak at 284.8 eV. Spectra were fitted using the CASA XPS software using Voigt-like peak shapes. Spin-orbit splitting ratios and splitting energies are constrained to obtain physically meaningful fits, using the NIST XPS database[3]

Scanning electron microscopy (SEM) imaging

SEM imaging and energy dispersive X-ray spectroscopy (EDX) analysis were performed using the FEI/Thermofisher Quanta 650 field emission gun SEM at the University of Manchester. The SEM

was equipped with a Bruker X Flash 6 | 30 silicon drift detector with Bruker ESPRIT EDX software v2.2. For high-resolution imaging, beam deceleration was employed to achieve a landing energy of 1 kV. For EDX analysis, beam conditions were set to 15 kV. High-angle annular dark-field scanning transmission electron microscopy (HAADF-STEM) images and EDX elemental maps were collected on a Thermo Fisher Titan STEM (G2 80-200) equipped with a Cs probe corrector (CEOS), high-angle annual dark-field (HAADF) detector and ChemiSTEM Super-X EDX detector, operating at 200 kV.

Synthesis of Ce-bptc

Typically, 5.0 mg of biphenyl-3,3',5,5'-tetracarboxylic acid was dissolved in 1.2 mL DMF, then 0.4 mL 0.533 M $(NH_4)_2Ce(NO_3)_6$ aqueous solution was added to the DMF solution, and the mixture was heated at 60 ℃ for 15 minutes. The resulted participate was washed by DMF and acetone three times and dried in the air. Yield: 35% (calculation based on cerium salt in the reaction). Analytically calculated (Found) for $\{Ce_6O_4(OH)_4(C_{16}H_6O_8)_3 \cdot (H_3O)_{1.6} \cdot 3DMF \cdot 10H_2O\}$ %: Ce, 35.3 (36.4); C, 28.8 (28.4); H, 2.87 (2.61); N, 1.76 (1.80).

Synthesis of Ce-UiO-66, Zr-UiO-66, and Zr-bptc

Synthesis and activation of Ce-UiO-66, Zr-UiO-66, and Zr-bptc were carried out using the reported methods.[4-6] The successful synthesis of these materials is characterized by PXRD and BET measurements.

Synthesis of Pd@Ce-bptc, Pd@Zr-bptc, Pd@Ce-UiO-66, Pd@Zr-UiO-66, Pd@CeO_2 and Pd@ZrO_2

The synthesis of the materials is based on the literature.[7] Typically, 200 mg of activated material was suspended in 20 mL n-hexane, and the mixture was sonicated for 20 minutes until it became homogeneous. After being stirred for around 30 minutes, 0.16 mL of aqueous $Pd(NO_3)_2$ solution (50mg/mL) was slowly added dropwise during vigorous stirring. Subsequently, the resultant mixture was continuously stirred for 3 hours. When the stirring was stopped, the solid settled to the bottom of the tube was harvested from the supernatant fluid by decanting and simply drying in air at room temperature. Then the dried powder was reduced under 5%H_2/Ar for 2 hours under 150 ℃. Other catalysts were prepared using the same method except with different supports.

Catalysis procedure

Typically, 5 mg of catalyst and magnetic stir bar were placed in a Schlenk tube, and the gas in the glass tube was replaced by H_2 three times. Then, 2.5 mL of THF, 1 mmol of phenylacetylene, and 1 mmol of mesitylene were injected into the Schlenk tube, and the mixture was stirred at 700 rpm under an atmospheric H_2 balloon and 25 ^oC. The reaction products were analysed by GC and GC-MS. For recycle test, the reaction condition is the same as the typical reaction conditions except for using the recycled catalyst. The conversion and selectivity were determined by GC-FID using mesitylene as the internal standard.

Structure determination and refinements of Synchrotron PXRD data.

Synchrotron PXRD measurements were conducted at Beamline I11 Diamond Light Source (Oxford, UK) [λ = 0.826562(2) Å]. Desolvated Ce-bptc was prepared by heating the as-synthesised sample at 60 ºC under vacuum for 1 day. To prepare the substrate-loaded samples, a drop of phenylacetylene was added into the desolvated MOF (0.05 mmol). After being soaked for 10 hours, the powder sample was loaded in a 0.7 mm borosilicate glass capillary to prevent preferred orientations. High-resolution synchrotron PXRD data were collected in the 2θ range of 0-150° with a step size of 0.001° using multi-analyser crystal (MAC) detectors at 25.0 °C.

TOPAS 5 was used to perform Pawley and Rietveld refinement on the PXRD patterns. Background, cell parameters and peak profile with Stephen model were first refined using Pawley refinement and then transferred to Rietveld refinement. The scale factor and lattice parameters were allowed to refine for all the diffraction patterns. The refined structural parameters include the fractional coordinates (x, y, z), the isotropic displacement factors for all the atoms, and the site occupancy factors (SOF) for the framework and guest molecules. The final stage of Rietveld refinement involved soft restraints to the C–C bond lengths within the benzene rings, and rigid body refinement was applied to the guest molecules in the pore. The quality of the Rietveld refinements was confirmed by the low weighted profile factors and the good fit to the data with reasonable isotropic displacement factors within experimental error

EPR measurement

Continuous wave EPR measurements were carried out at X-band (9.85 GHz) using an EMX Micro spectrometer (Bruker). Modulation amplitude of 0.9 mT was used with a microwave power of ~ 2.0 mW based on spectral lines saturation test. Strong pitch (g = 2.0028) was used as a standard reference.

Theoretical modelling of EPR spectra was performed using the Easyspin toolbox package (Version 6.0.0) in MATLAB software (version R2020a).

All reagents were deoxygenated under Ar. For the in situ EPR measurements, α-phenyl N-tertiary-butyl nitrone (PBN) was dissolved in THF (0.2 mol/L) and used as a spin trap. Phenylacetylene (0.05 mmol), Pd@Ce-bptc (10 mol%, 0.005 mmol) were mixed in the THF solution (3 mL) in a deoxygenated vial under Ar, followed by 0.1 mL of the PBN stock solution. 0.5 mL of the resultant PBN mixed solution was then transferred into a capillary for freeze pumping to further degas the solution in order to fully remove all the dissolved gases. (<0.01 mbar). The capillary was then connected to a H_2 gas bag and directly used for EPR measurements. In situ EPR spectra of the reactions were collected before and after connected to the H_2 gas bag, the reference experiment was conducted without adding the substrate.

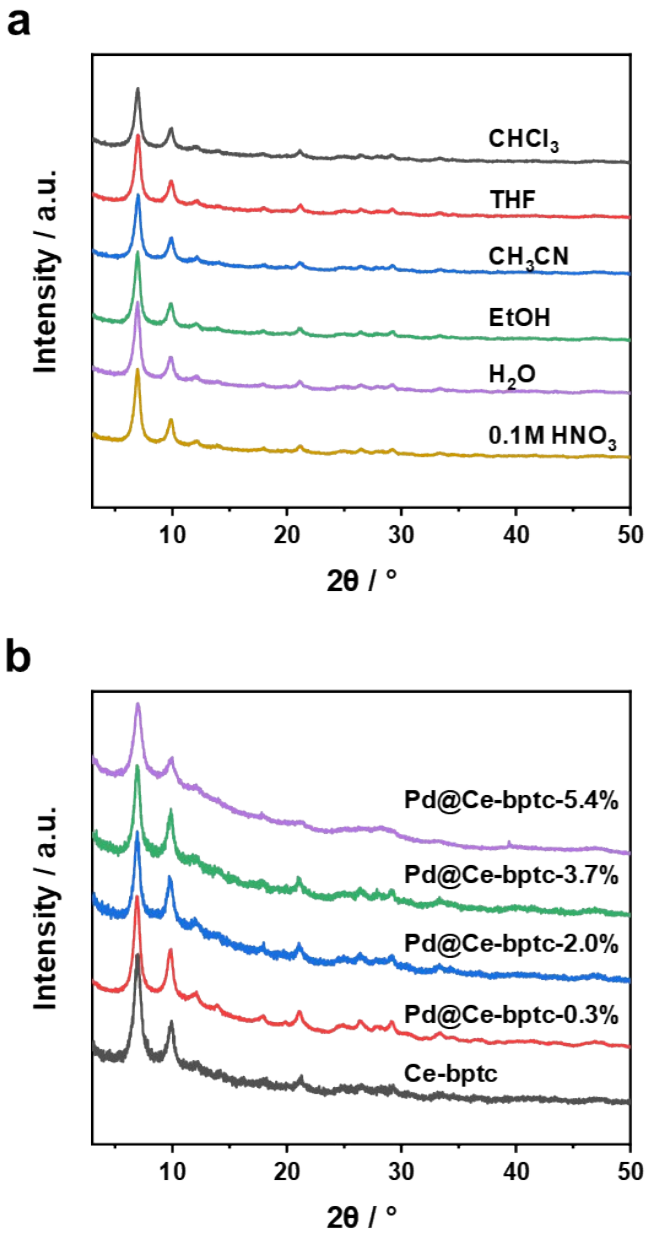

Figure S1 PXRD patterns on MOF stability test. (a) Stability of Ce-bptc soaked in different solvents for 24 hours; (b) Stability with different amount of Pd loading.

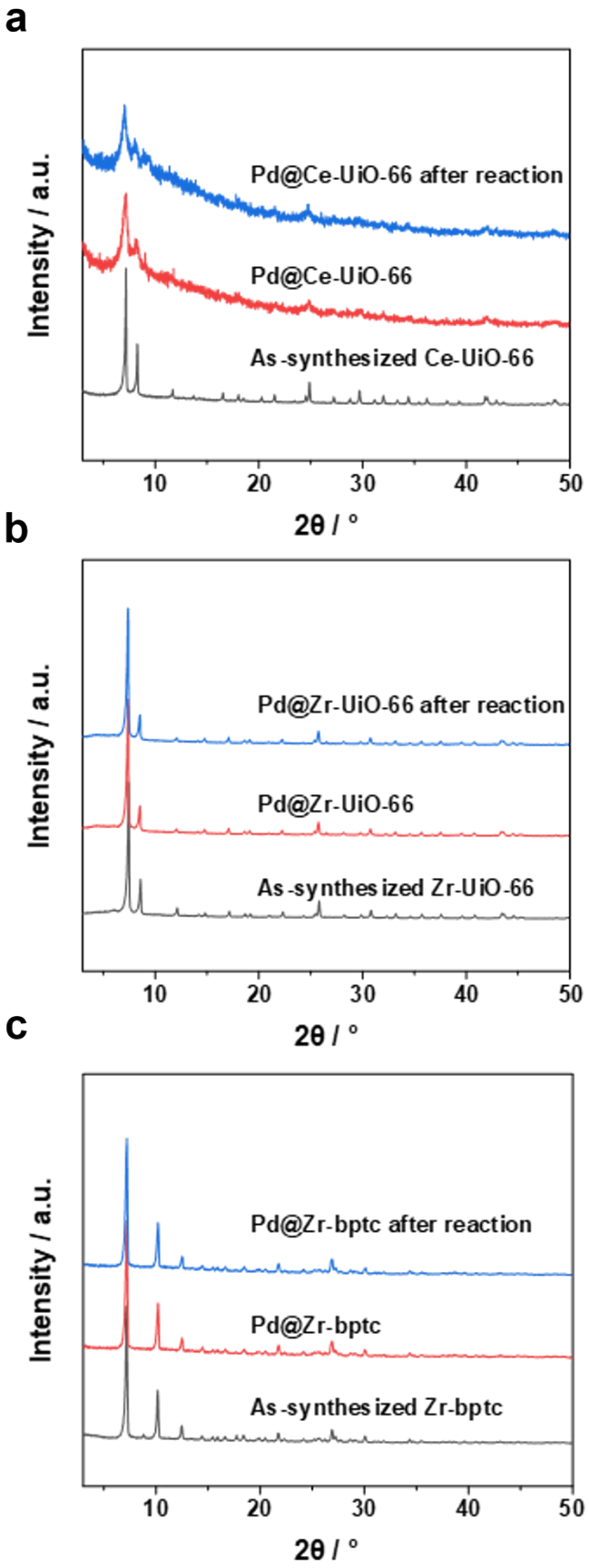

Figure S2 PXRD patterns of (a) Pd@Ce-UiO-66, (b) Pd@Zr-UiO-66, (c) Pd@Zr-bptc before and after Pd loading and after the reaction.

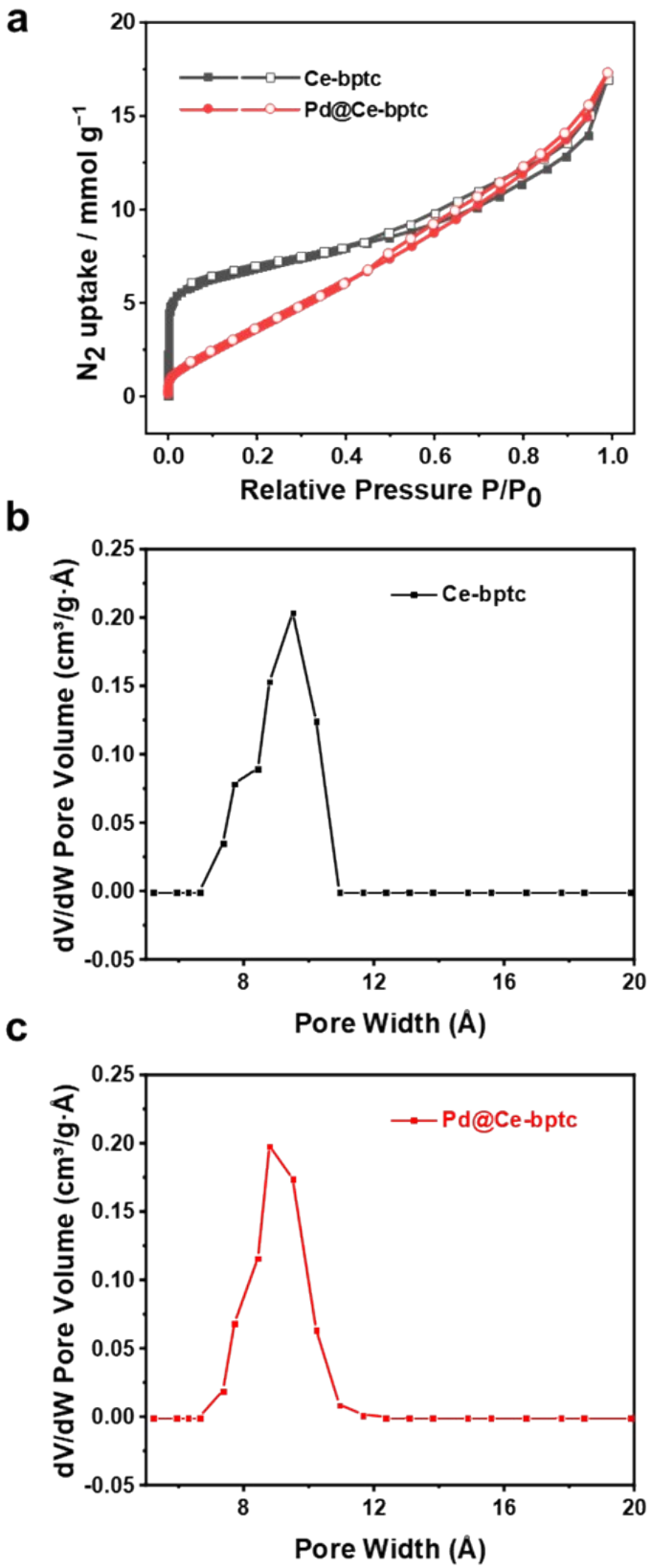

Figure S3 (a) N_2 isotherms at 77 K and pore size distribution of (b) Ce-bptc and (c) Pd@Ce-bptc.

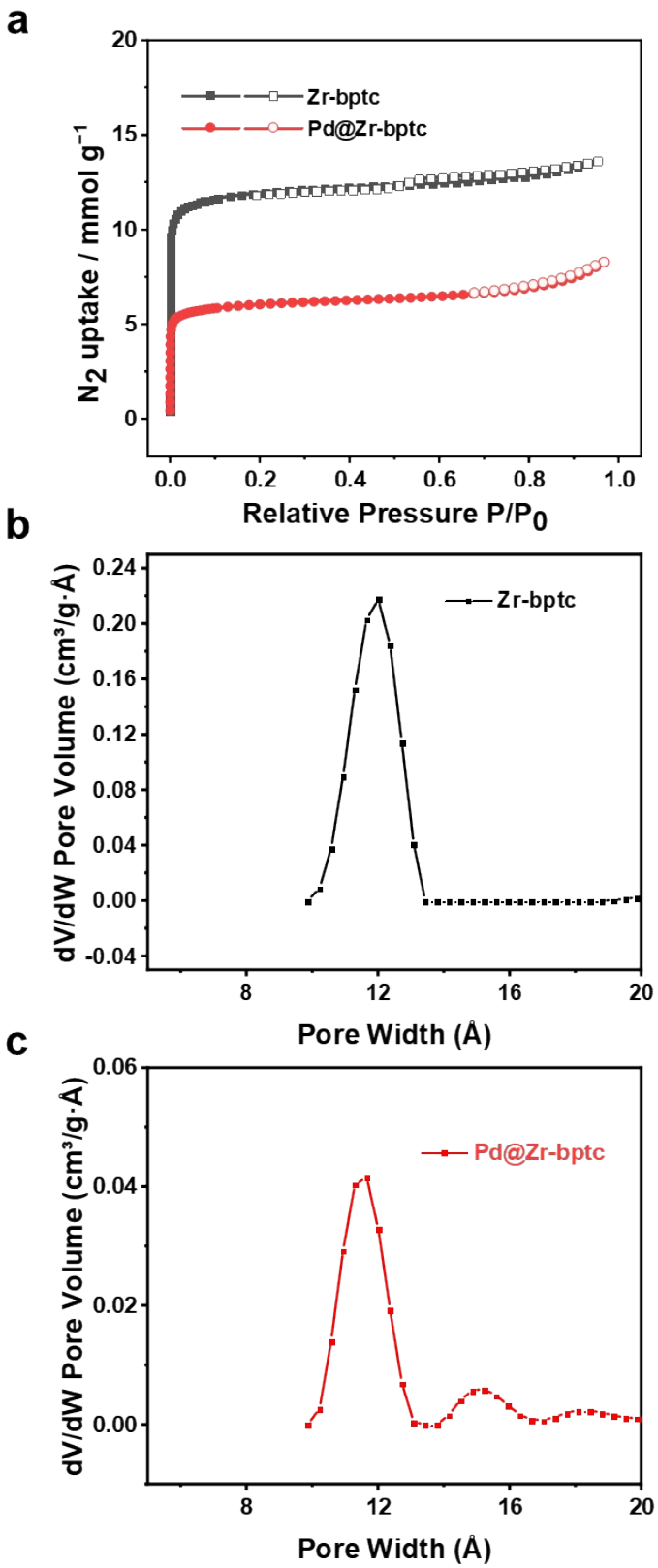

Figure S4 (a) N_2 uptake at 77 K and pore size distribution of (b) Zr-bptc and (c) Pd@Zr-bptc.

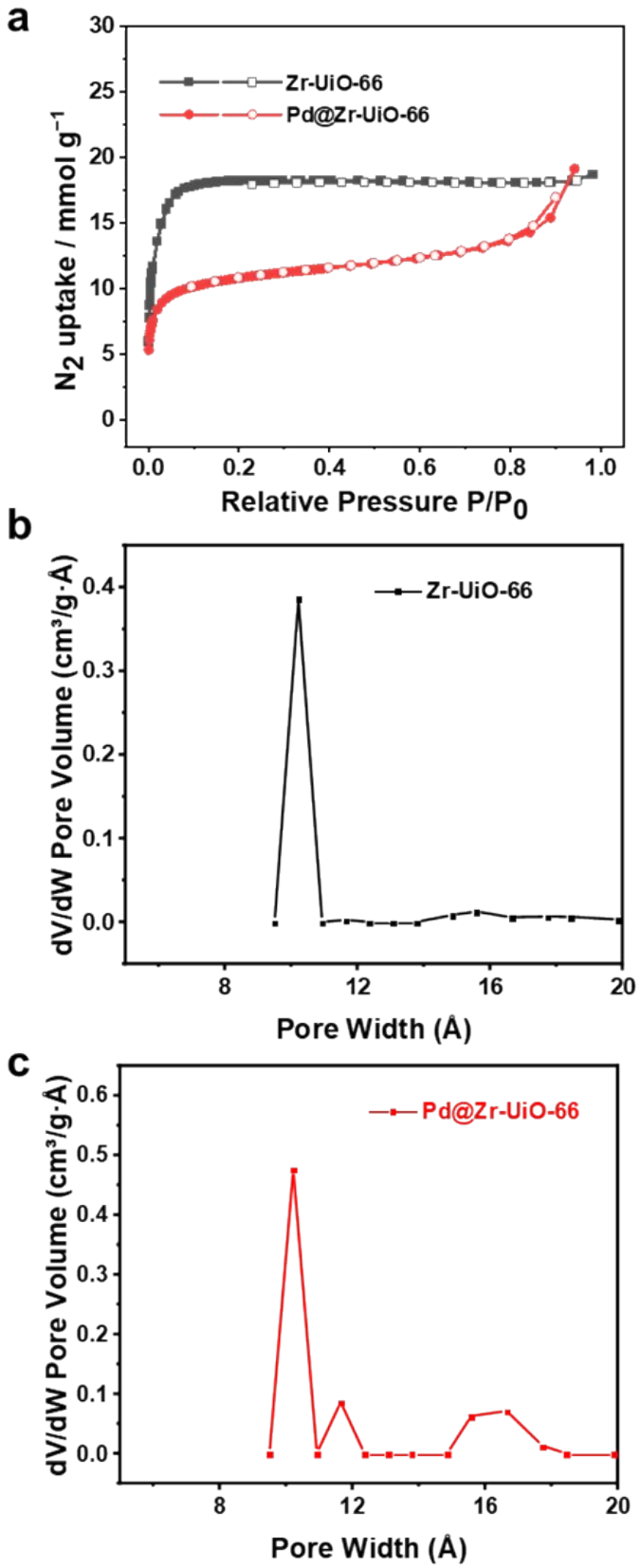

Figure S5 (a) N_2 uptake at 77 K and pore size distribution of (b) Zr-UiO-66 and b) Pd@ Zr-UiO-66.

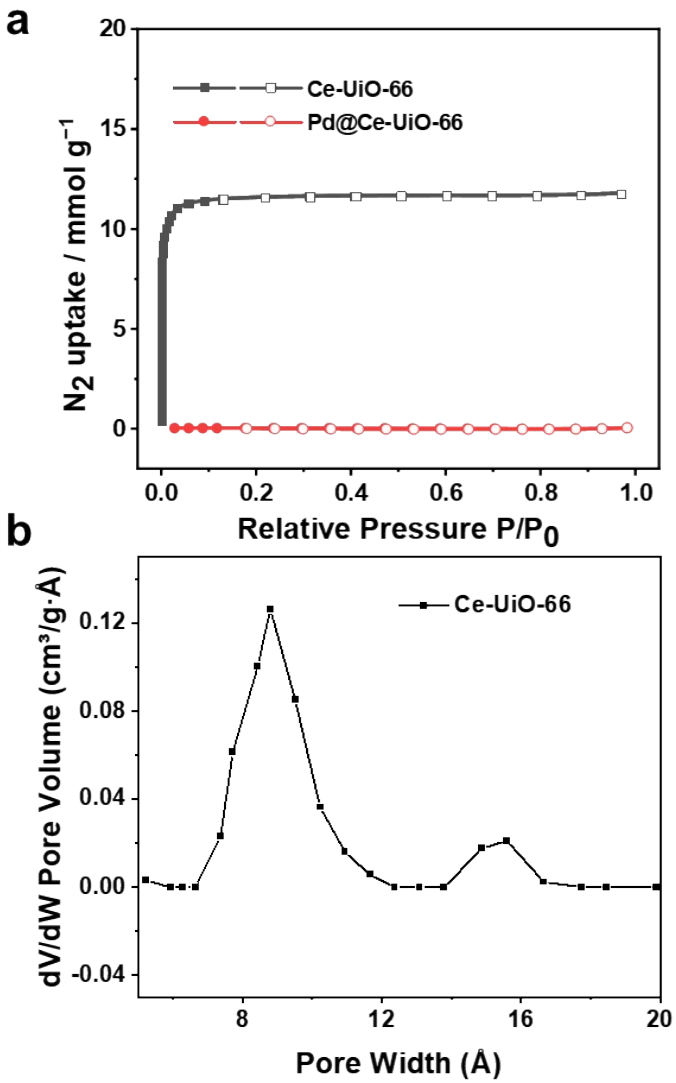

Figure S6 (a) N_2 uptake at 77 K of Ce-UiO-66 and Pd@Ce-UiO-66. Pore size distribution of (a) Ce-UiO-66.

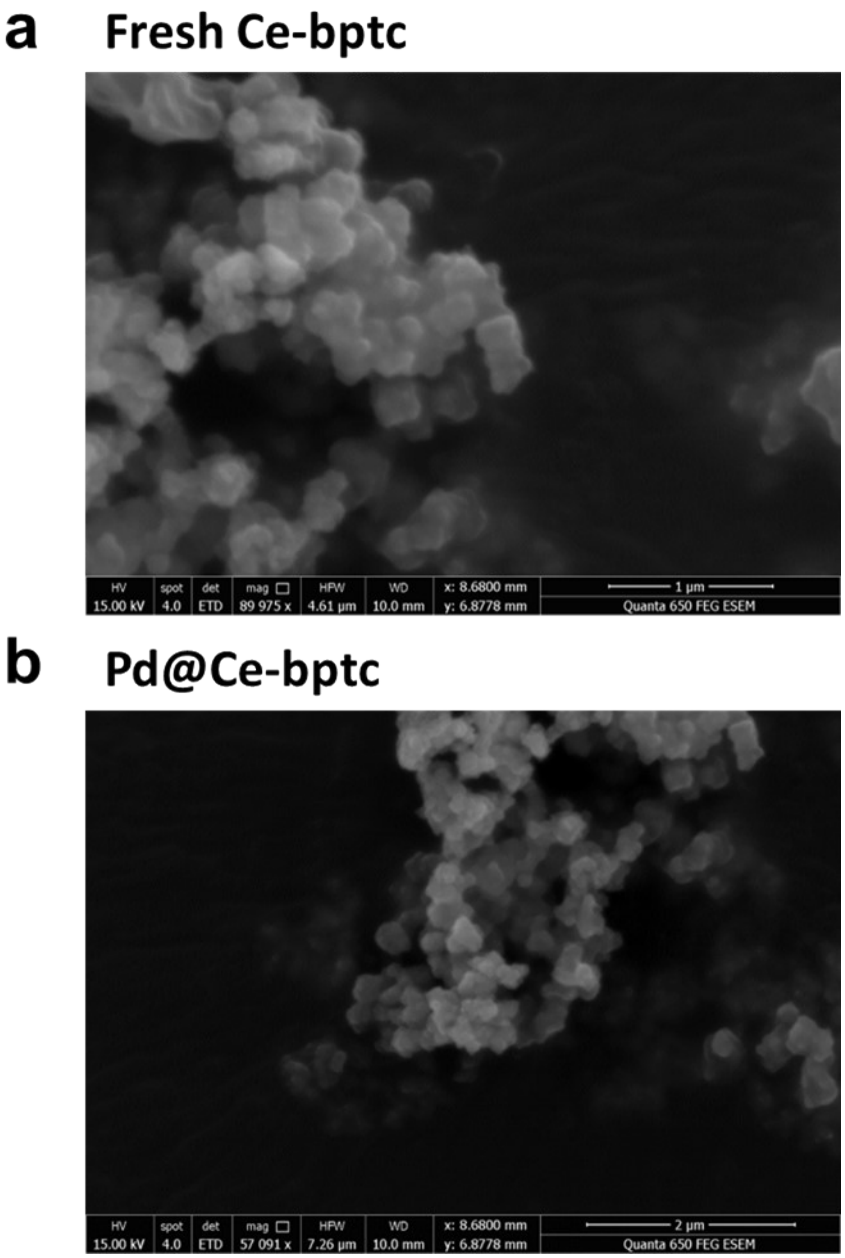

Figure S7 SEM images of (a) Ce-bptc and (b) Pd@Ce-bptc.

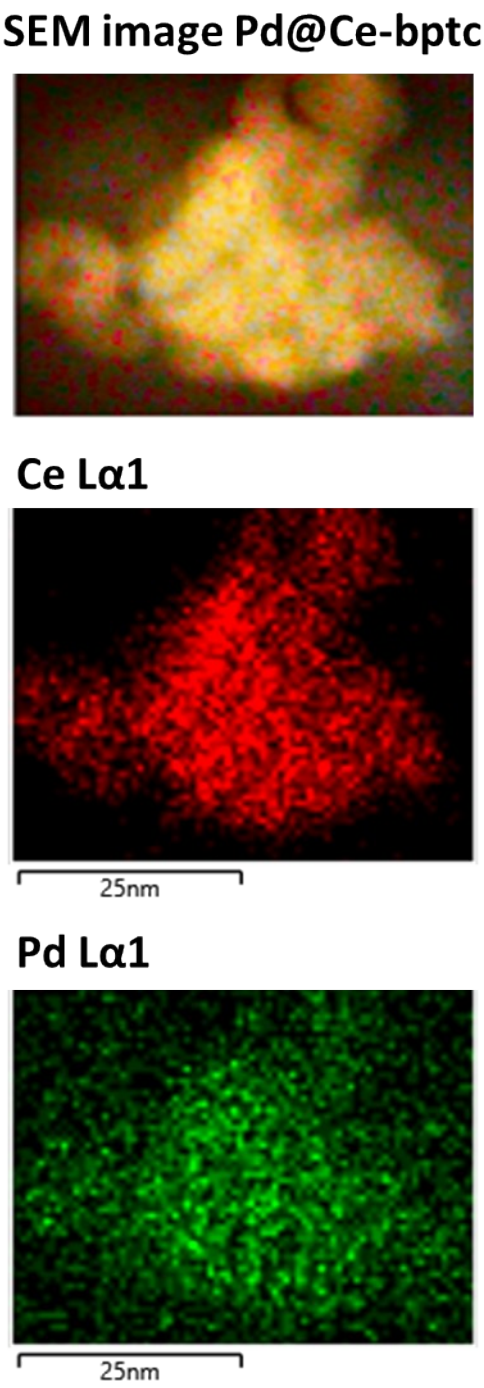

Figure S8 EDX mapping of Pd@Ce-bptc.

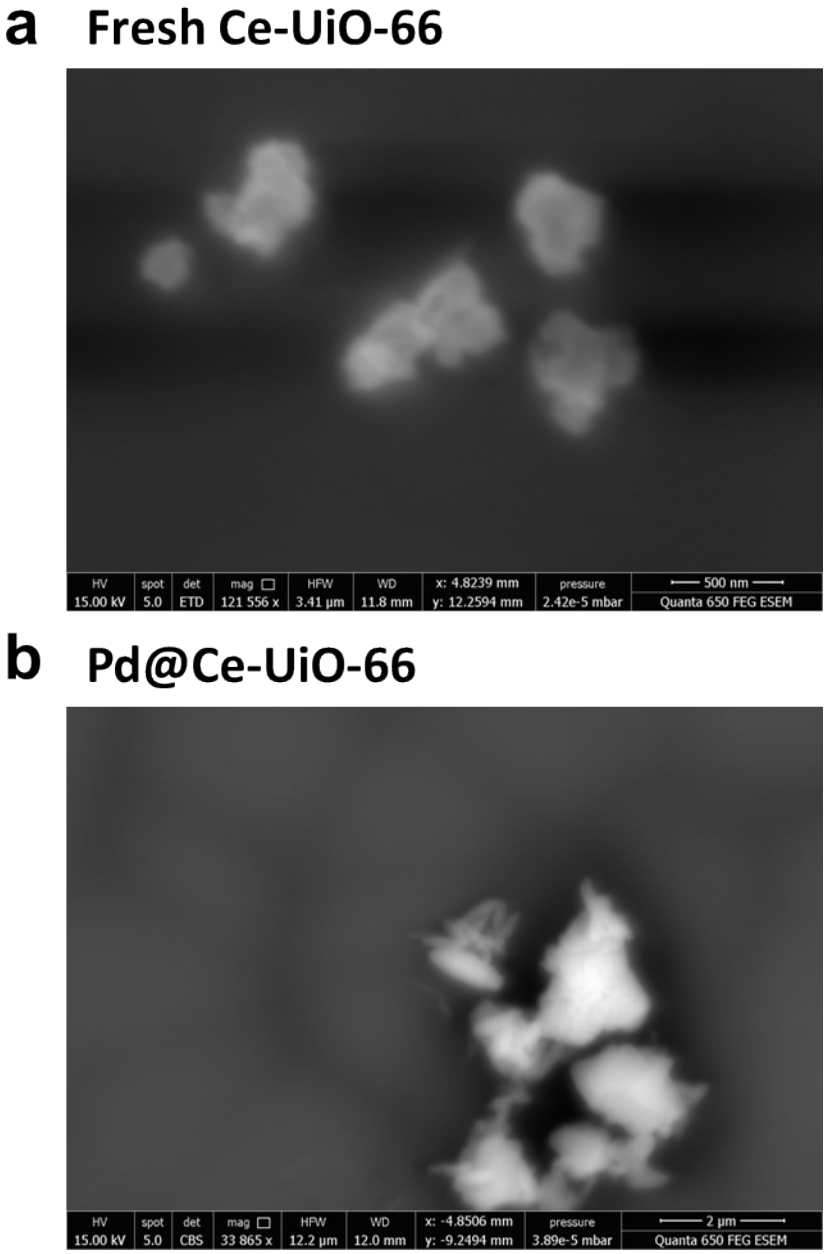

Figure S9 SEM images of (a) Ce-UiO-66 and (b) Pd@Ce-UiO-66.

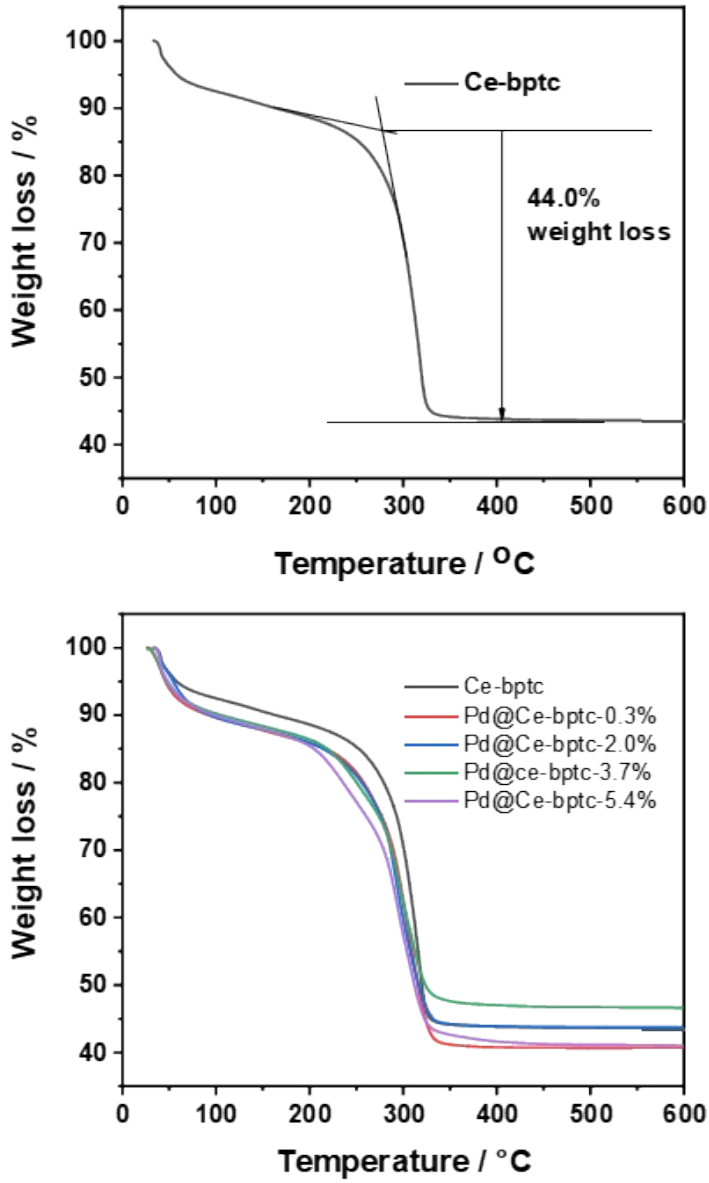

Figure S10 TGA results of (a) Ce-bptc and (b) Pd@Ce-bptc.

The first weight loss (12.3%) below 200 ℃ corresponds to the removal of adsorbed solvent molecules in the pores of the MOF. The second weight loss (44.0%) at 250-400 ℃corresponds to the decomposition of the MOF: 47.9% weight loss from $Ce_6O_4(OH)_4$ $(BPTC)_3(H_3O)_{1.6}$ to $(CeO_2)_6$.

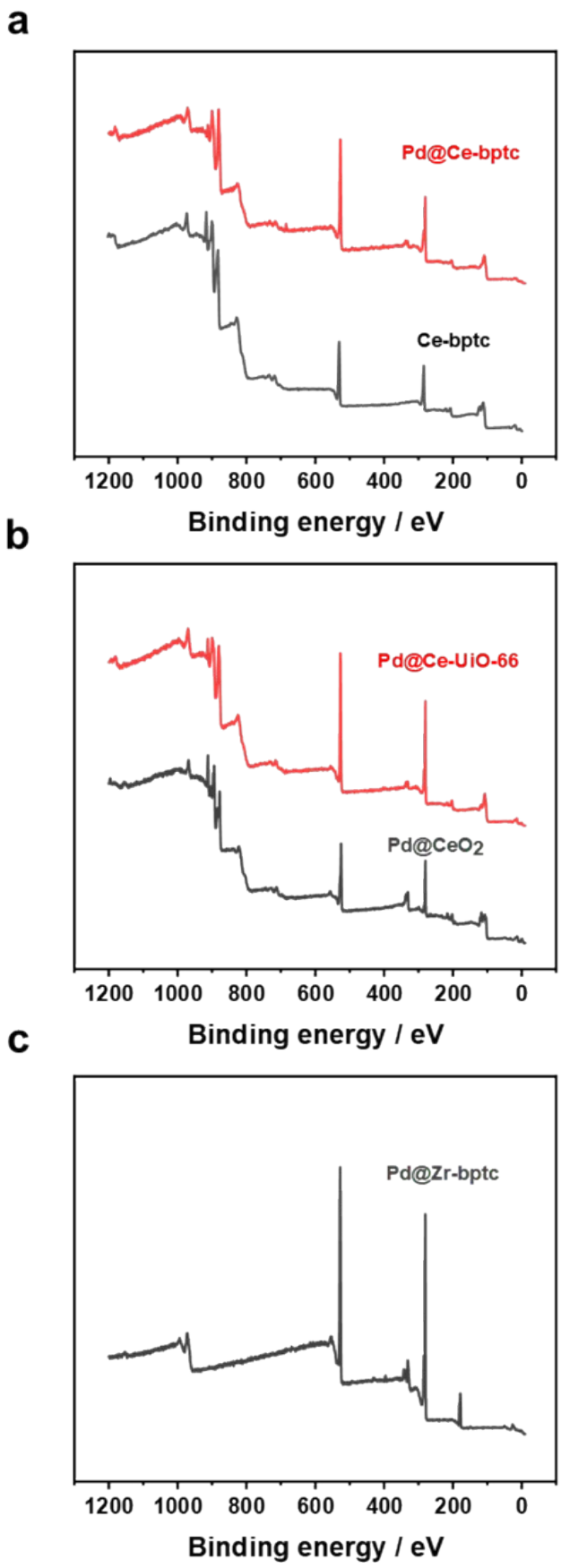

Figure S11 XPS spectra of (a) Ce-bptc, Pd@Ce-bptc, (b) Pd@Ce-UiO-66, and Pd@CeO_2, and (c) Pd@Zr-bptc.

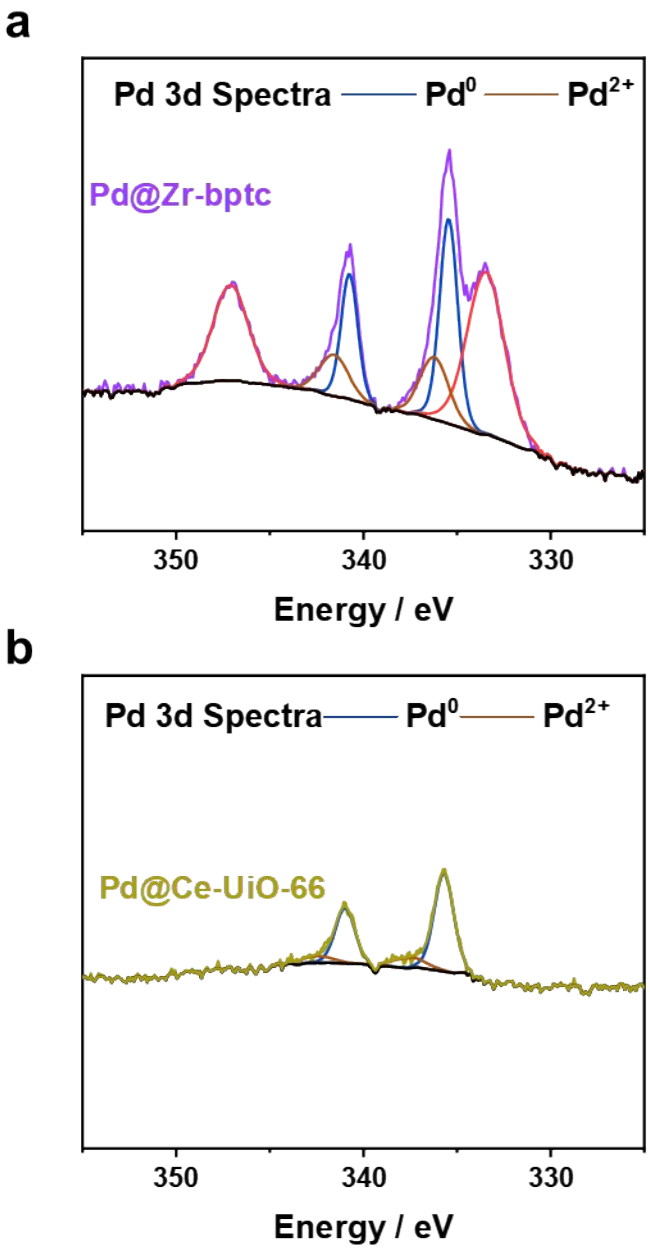

Figure S12 XPS Pd 3d spectra of (a) Pd@Zr-bptc, and (b) Pd@Ce-UiO-66. The spectrum in (a) contains overlapping peaks of Zr 3p (red lines).

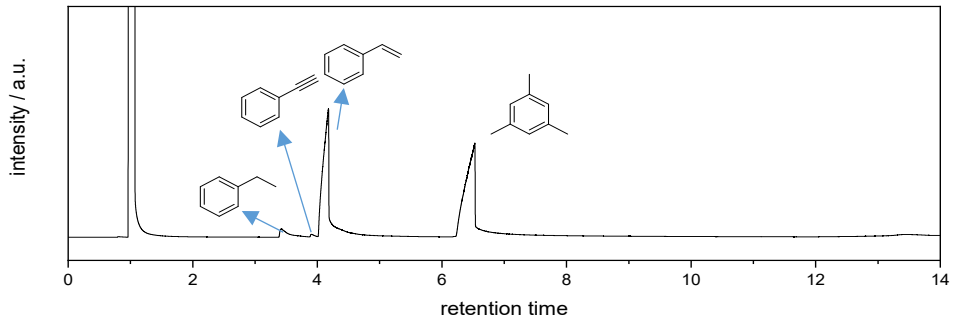

Figure S13 The GC analysis of the liquid mixture of the phenylacetylene semihydrogenation reaction. Reaction condition: 5 mg MOF, 1 mmol phenylacetylene, 1 mmol mesitylene, 2 mL THF, 25°C, 2.5h.

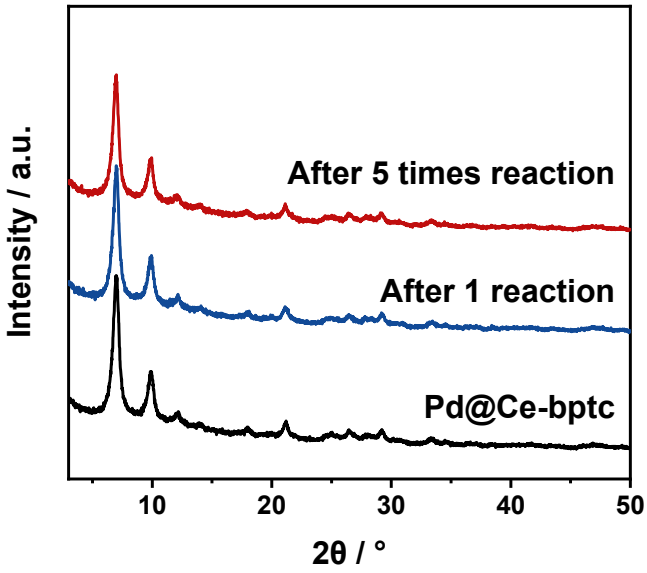

Figure S14 PXRD patterns of as-synthesised and used Pd@Ce-bptc catalysts.

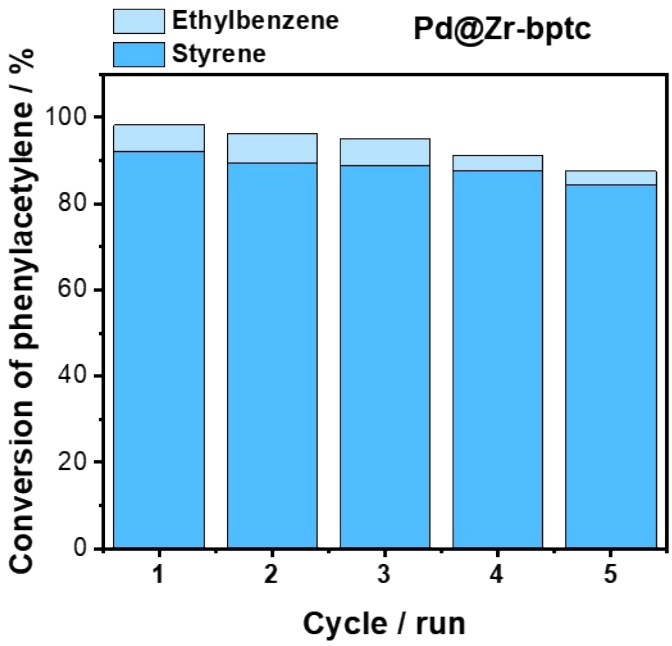

Figure. S15 Recyclability test of phenylacetylene semihydrogenation reaction using Pd@Zr-bptc Reaction condition: 5mg MOF, 1mmol phenylacetylene, 1mmol mesitylene, 2mL THF, 25^{o}C, 2.5h.

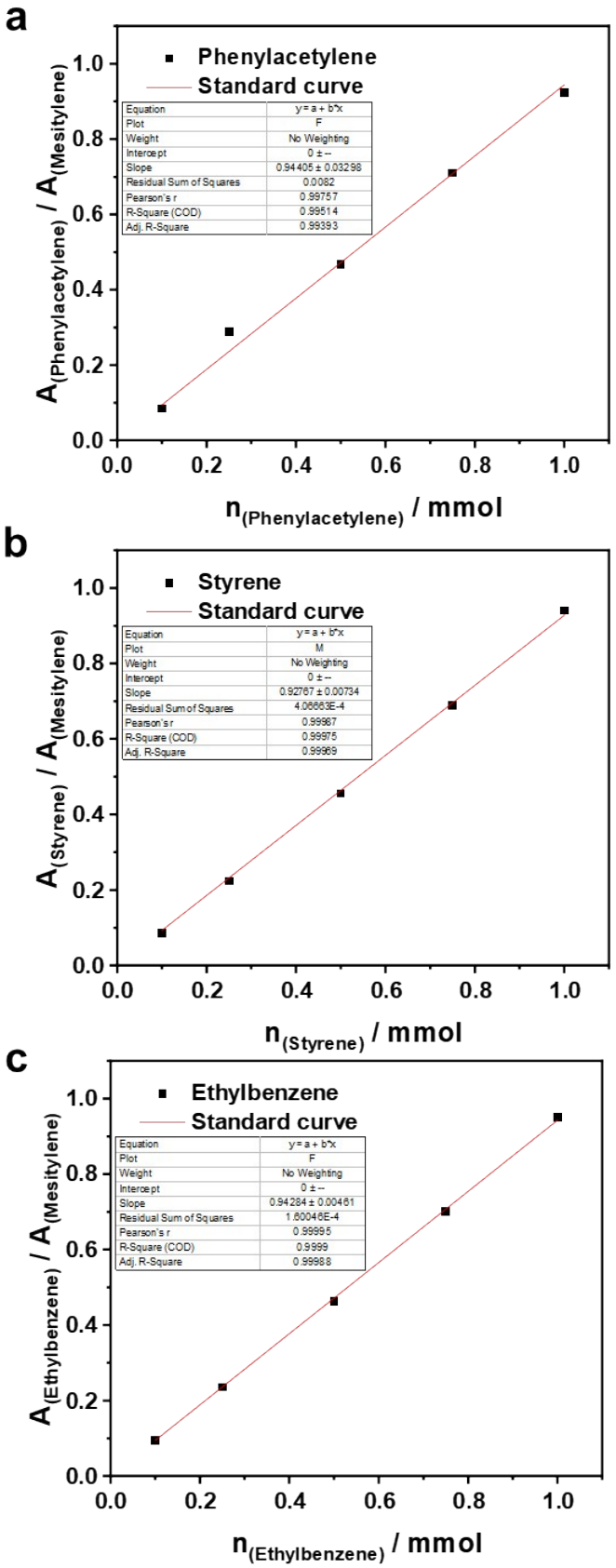

Figure S16 GC-FID standard curve of (a) Phenylacetylene, (b) Styrene, and (c) Ethylbenzene.

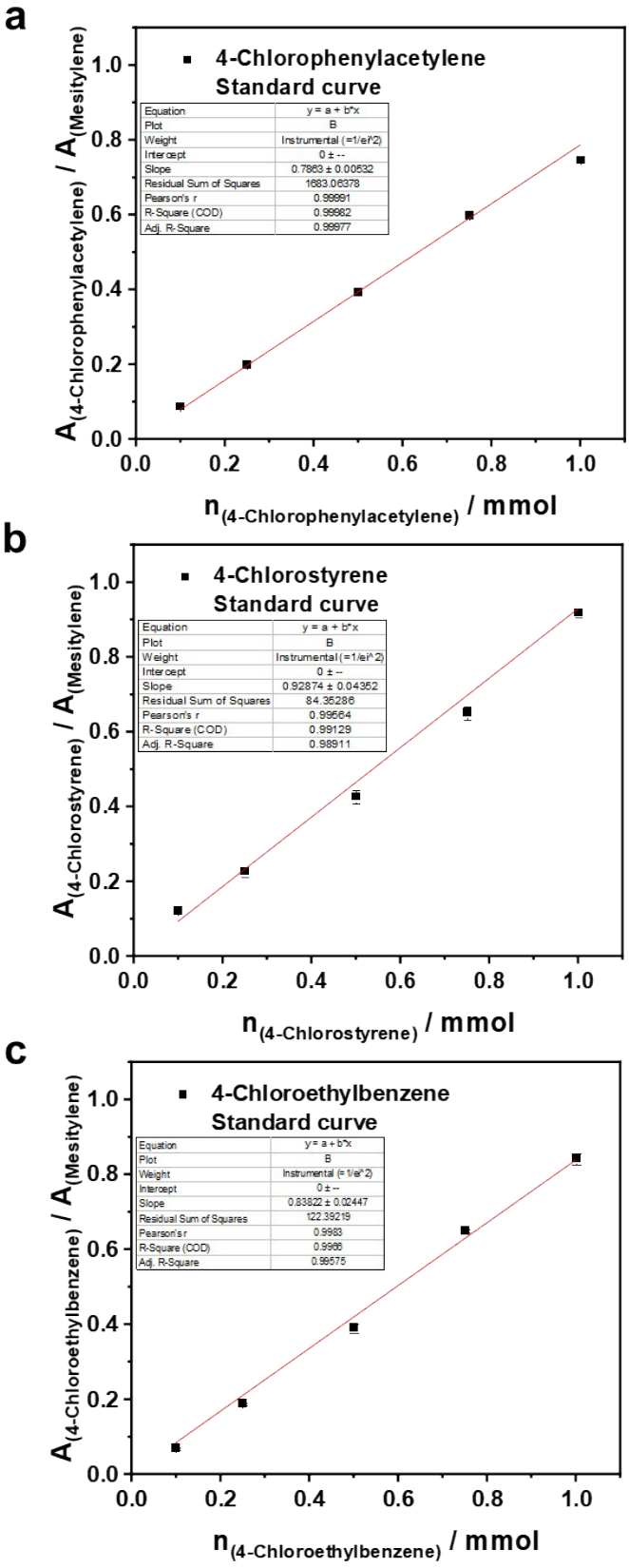

Figure S17 GC-FID standard curve of (a) 4-Chlorophenylacetylene, (b) 4-Chlorostyrene, and (c) 4-Chloroethylbenzene.

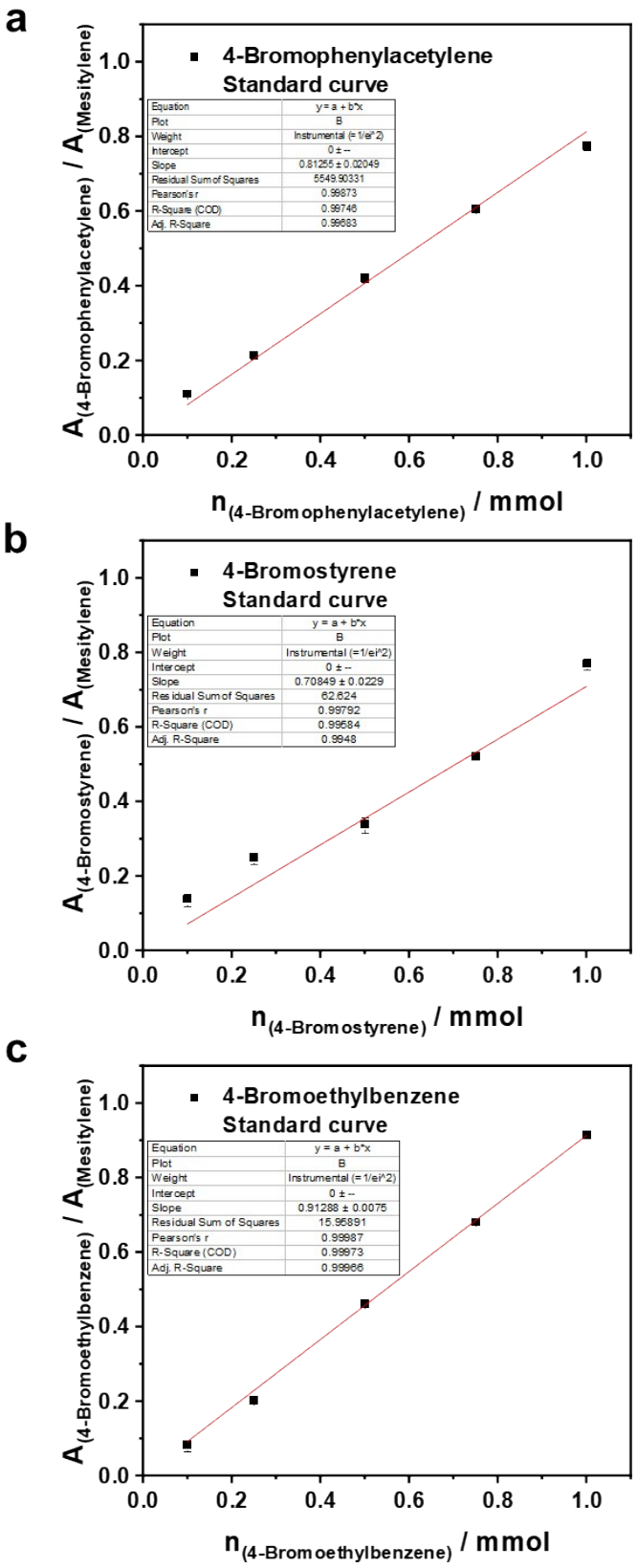

Figure S18 GC-FID standard curve of (a) 4-Bromophenylacetylene, (b) 4-Bromostyrene, and (c) 4-Bromoethylbenzene.

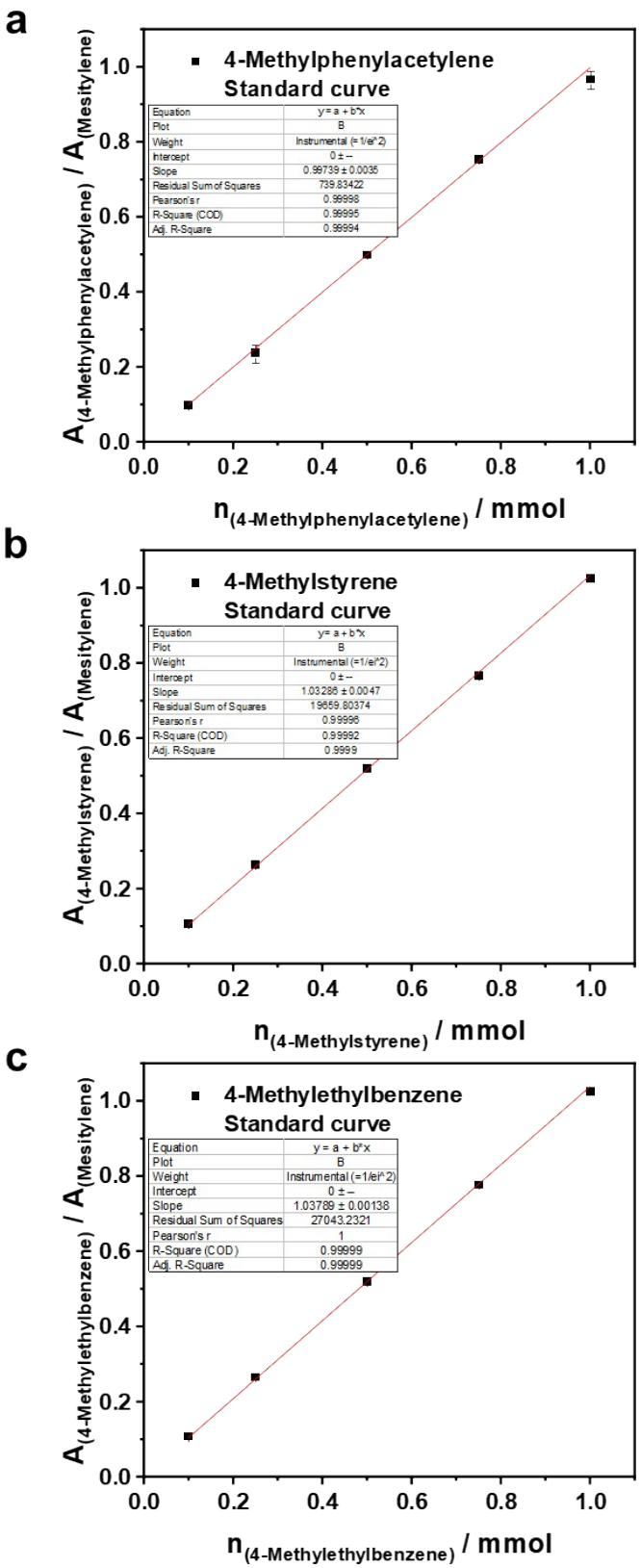

Figure S19 GC-FID standard curve of (a) 4-Methylphenylacetylene, (b) 4-Methylstyrene, and (c) 4-Methylethylbenzene.

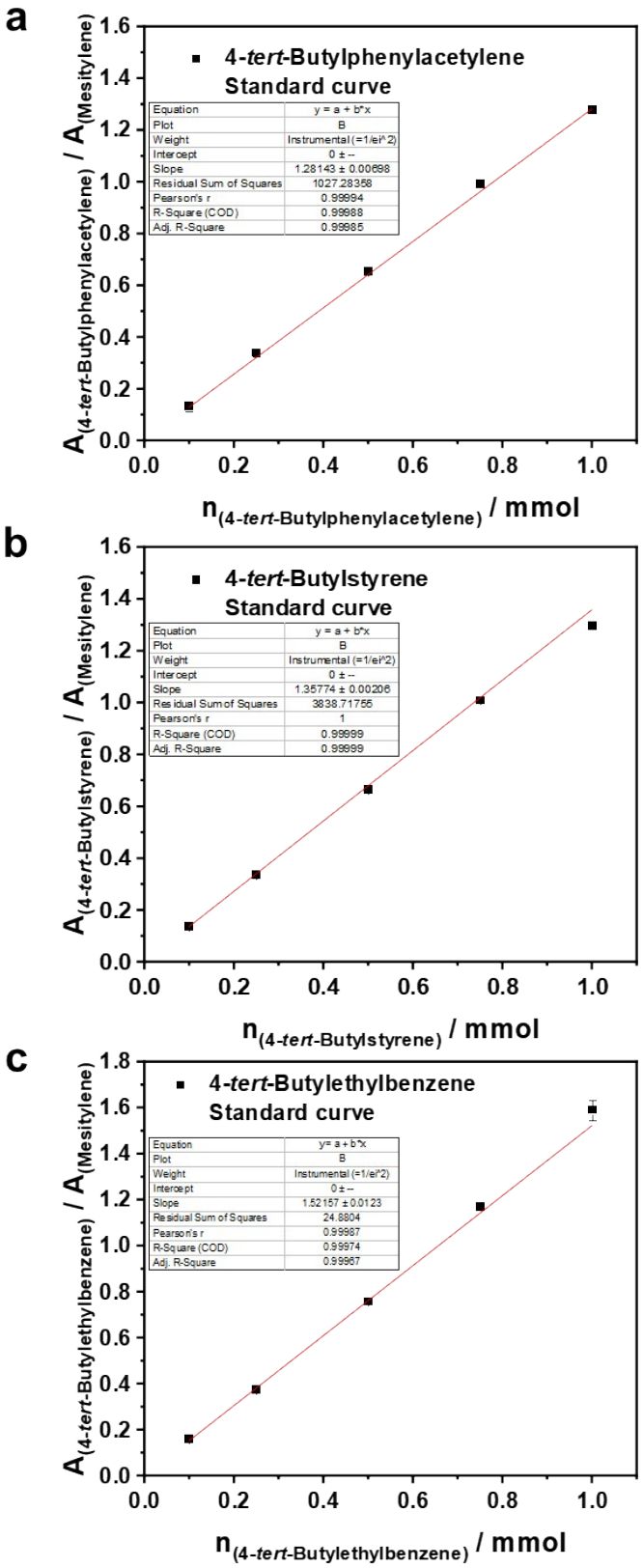

Figure S20 GC-FID standard curve of (a) 4-*tert*-Butylphenylacetylene, (b) 4-*tert*-Butylstyrene, and (c) 4-*tert*-Butyl ethylbenzene.

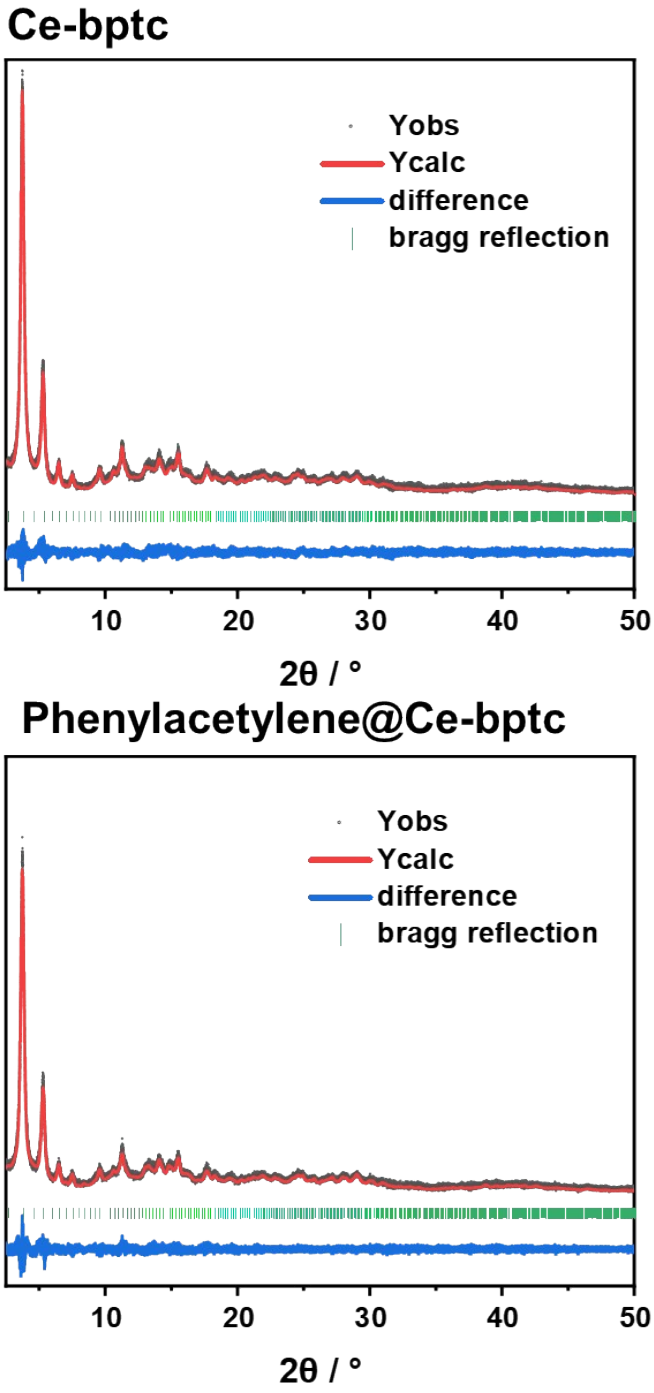

Figure S21 Synchrotron PXRD pattern of Ce-bptc and phenylacetylene loaded Ce-bptc. Experimental data shown in black, Rietveld refinement model in red, difference pattern in blue.

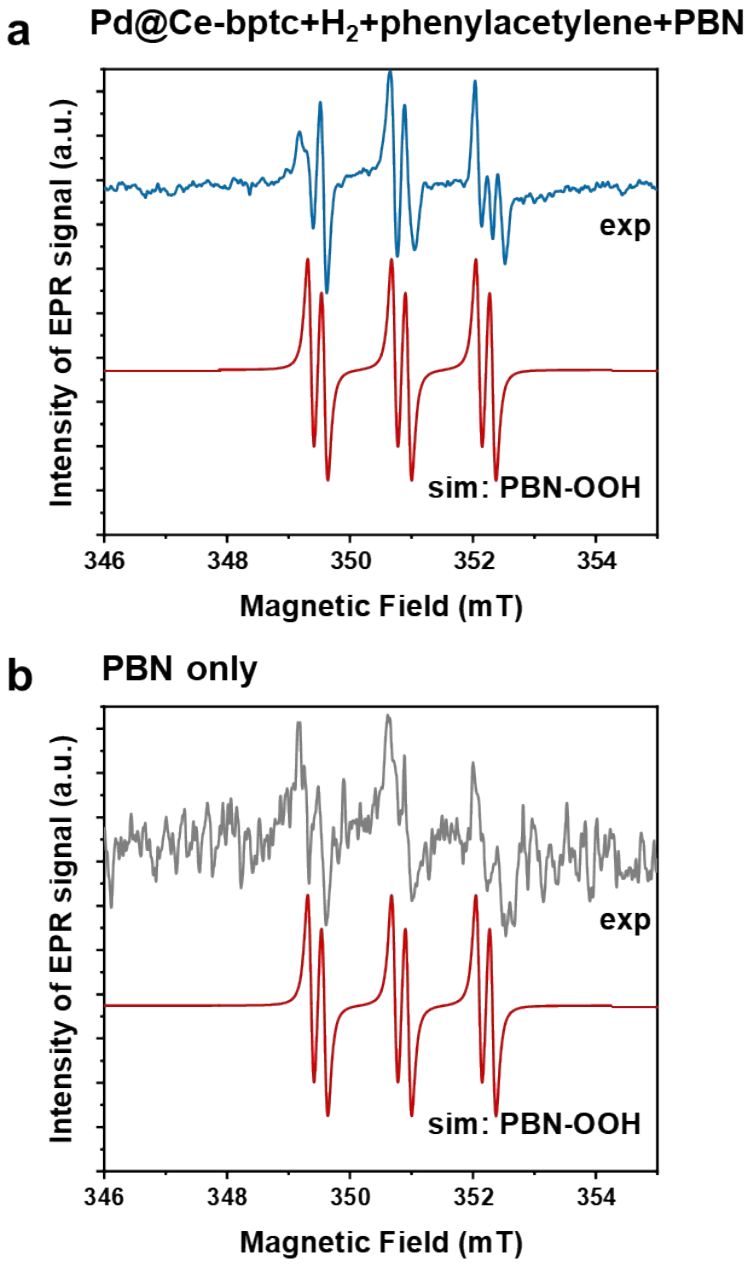

Figure S22 *In situ* X-band EPR spectra under controlled conditions using PBN as spin trap. Experiment and simulated spectra of (a) Pd@Ce-bptc + H_2 + phenacetylene + PBN and (b) PBN in THF solution, both of them showing weak peak of PBN-OOH radical.

Table S1 Crystallography data for Ce-bptc and Phenylacetylene@ Ce-bptc.

Sample Name	Ce-bptc	Phenylacetylene@ Ce-bptc
CCDC number	2205374	2205379
Crystal system	Cubic	Cubic
Space Group	*Im*-3	*Im*-3
Formula	$Ce_6O_4(OH)_4(bptc)_3$	$Ce_6O_4(OH)_4(bptc)_3(C_8H_6)_{0.75}$
a (Å)	25.1845(7)	25.2406(7)
beta (°)	90	90
Cell Volume /Å^3	15973.5(14) Å^3	16080.6(14) Å^3
Cell density g/cm^3	1.739	1.734
Method	Rietveld	Rietveld
R_{wp} (%)	7.226	7.184
R_{exp}(%)	3.868	4.117
GOF	1.868	1.745

Table S2 the parameter of spintrap experiment of Pd@Ce-bptc.

	Adducts	**g factor**	**$A^{14}N$ / G**	**$A^{\alpha}H1$ / G**	**$A^{\alpha}H2$ / G**	**lw/mT**	**Weighting**
Pd@Ce-bptc+H_2+PBN	PBN-H	2.0055	15.0	7.4	7.4	0.50 0.20	0.89
	PBN-OOH	2.0060	13.7	2.3	/	0.0 0.18	0.11
Pd@Ce-bptc+H_2+substrate+PBN	PBN-OOH	2.0060	13.7	2.3	/	0.06 0.15	1.00
PBN (0.4 M THF solution)	PBN-OOH	2.0060	13.7	2.3	/	0.06 0.15	1.00

Table S3 Comparison of the catalytic activity with reported materials.

No.	Catalysts	Temp (°C)	$P(H_2)$ (bar)	T (h)	Conv. (%)	Sel. of alkene (%)	TOF (h^{-1})	Cycle tests	Ref
1	Pd@Ce-bptc	25	1	2.5	99	93	396	Conv.: 1st 99%-5th 97% Sel.: 1st 92%-5th 94%	This work
2	Pd@Zr-bptc	25	1	2.5	99	91	391	Conv.: 1st 99%-5th 88% Sel.: 1st 92%-5th 96%	This work
3	Pd@Ce-UiO-66	25	1	3	99	88	353		This work
4	Pd@Zr-UiO-66	25	1	6	99	71	122		This work
5	Pd-Pb(27%) alloy NCs	25	1	7.5	99	91			8
6	Lindlar catalyst	40	1	23.3	100	88	30		9
7	Fe_3O_4@ZIF-8/Pd	40	1	4.5	100	91	154	Conv.:1st 100%-5th 100% Sel.: 1st 93%-5th 93% at 1.67h	9
8	$PdZn_{0.6}/Al_2O_3$	40	1	2.1	100	86	4318	Conv.: 1st 92%-5th 92% Sel.: 1st 91%-5th 89%	10
9	Pd NCs@NCM	25	1	5	99	95	380	After 24 h reaction: Sel.: 87%	11
10	Pd/ZnO@C	30	1	1	96	99	733	Conv.: 1st 96%-5th 96% Sel.: 1st 99%-5th 99%	12

11	Pd@MPSO/SiO_2-1	30	1	2	99	97	248	Conv.: 1st 99%-5th 99% Sel.: 1st 97%-5th 97%	13
12	Pd/pph3@FDU-12	25	1	8	92	94	560		14
13	Pd@mpg-C_3N_4	30	1	1.4	99	94	771	Conv.: 1st 95%, 70 min-9th 85%, 140 min Sel.: 1st 95%-9th 96%	15
14	Pd+PEI@HSS	30	1	4.5	99	91	44		16
16	Pd/IL/$Cu(BTC)_3$	30	1	0.6	99	99	2287	Conv.: 1st 99%-5th 95% Sel.: 1st 99%-5th 99%	17
17	Pd/NHPC-DETA-50	35	1	0.33	99	95	2872		18
18	1.3Pd–3.6Cu_2O/TiO_2	30	1	1.5	100	98	353		19
19	Pd@Ag-in-UiO-67	25	1	1.6	100	91	80		20

Reference:

1. P. Tignol, V. Pimenta, A.-L. Dupont, S. Carvalho, A. A. Mohtar, M. Inês Severino, F. Nouar, M. L. Pinto, C. Serre, B. Lavédrine, *Small Methods* 2024, **8**, 2301343.
2. D. Aulakh, T. Islamoglu, V. F. Bagundes, J. R. Varghese, K. Duell, M. Joy, S. J. Teat, O. K. Farha, M. Wriedt, *Chem. Mater.* 2018, **22**, 8332-8342.
3. NIST X-ray Photoelectron Spectroscopy Database, NIST Standard Reference Database Number 20, National Institute of Standards and Technology, Gaithersburg MD, 20899, 2000, DOI: https://dx.doi.org/10.18434/T4T88K.
4. M. Lammert, M. T. Wharmby, S. Smolders, B. Bueken, A. Lieb, K. A. Lomachenko, D. De Vosc, N. Stock, *Chem. Commun.* 2015, **51**, 12578-12581.
5. J. Cavka, S. Jakobsen, U. Olsbye, N. Guillou, C. Lamberti, S. Bordiga, P. Lillerud, *J. Am. Chem. Soc.* 2008, **42**, 13850–13851.
6. H. Wang, X. Dong, J. Lin, S. Teat, S. Jensen, J. Cure, E. Alexandrov, Q. Xia, K. Tan, Q. Wang, D. Olson, D. Proserpio, Y. Chabal, T. Thonhauser, J. Sun, Y. Han, J. Li, *Nat. Commun.* 2018, **9**, 1-11.
7. M. Yadava, Q. Xu, *Chem. Commun.*, 2013, **49**, 3327-3329.
8. W. Niu, Y. Gao, W. Zhang, N. Yan, X. Lu, *Angew. Chem. Int. Ed.* 2015, **28**, 8271-8274.
9. L. Yang, Y. Jin, X. Fang, Z. Cheng, Z. Zhou, *Ind. Eng. Chem. Res.* 2017, **48**, 14182-14191.
10. Z. Wang, L. Yang, R. Zhang, L. Li, Z. Cheng, Z. Zhou, *Catal. Today* 2016, **264**, 37-43.
11. X. Li, Y. Pan, H. Yi, J. Hu, D. Yang, F. Lv, W. Li, J. Zhou, X. Wu, A. Lei, L. Zhang, *ACS Catal.* 2019, **5**, 4632-4641.
12. H. Tian, F. Huang, Y. Zhu, S. Liu, Y. Han, M. Jaroniec, Q. Yang, H. Liu, G. Q. M. Lu, J. Liu, *Adv. Funct. Mater.* 2018, **32**, 1801737.
13 T. Mitsudome, Y. Takahashi, S.; Ichikawa, T. Mizugaki, K. Jitsukawa, K. Kaneda, *Angew. Chem. Int. Ed.* 2013, **5**, 1481-1485.
14. M. Guo, H. Li, Y. Ren, X. Ren, Q. Yang, C. Li, *ACS Catal.* 2018, **7**, 6476-6485.
15. D. Deng, Y. Yang, Y. Gong, Y. Li, X. Xu, Y. Wang, *Green Chem.* 2013, **9**, 2525-2531.
16. Y. Kuwahara, H. Kango, H. Yamashita, *ACS Catal.* 2019, **3**, 1993-2006.
17. L. Peng, J. Zhang, S. Yang, B. Han, X. Sang, C. Liu, G. Yang, *Green Chem.* 2015, **8**, 4178-4182.
18. Q. Luo, Z. Wang, Y. Chen, S. Mao, K. Wu, K. Zhang, Q. Li, G. Lv, G. Huang, H. Li, Y. Wang, *ACS Appl. Mater. Interfaces.* 2021, **27**, 31775-31784.
19. J. Zhao, H. Zhang, F. Yan, H. Jia, Z. Li, J. Wang, *Catal. Sci. Technol.* 2021, **13**, 4539-4548.
20. L. Chen, B. Huang, X. Qiu, X. Wang, R. Luque, Y. Li, *Chem. Sci.* 2016, **1**, 228-233.